AGU PUBLICATIONS

Geophysical Research Letters

RESEARCH LETTER
10.1002/2016GL069273

Key Points:
- Multidecadal intrinsic oceanic variability is shown to have a substantial imprint in eddy-active regions
- Intrinsic oceanic variability is compared to the simulated internal climate variability from CMIP5 experiments
- A spectrum model for multidecadal variability is suggested from time series analysis

Correspondence to:
G. Sérazin,
guillaume.serazin@lgge.obs.ujf-grenoble.fr

Citation:
Sérazin, G., B. Meyssignac, T. Penduff, L. Terray, B. Barnier, and J.-M. Molines (2016), Quantifying uncertainties on regional sea level change induced by multidecadal intrinsic oceanic variability, *Geophys. Res. Lett.*, *43*, 8151–8159, doi:10.1002/2016GL069273.

Received 27 APR 2016
Accepted 28 JUL 2016
Accepted article online 1 AUG 2016
Published online 15 AUG 2016

Quantifying uncertainties on regional sea level change induced by multidecadal intrinsic oceanic variability

Guillaume Sérazin[1,2], Benoit Meyssignac[3], Thierry Penduff[1], Laurent Terray[2], Bernard Barnier[1], and Jean-Marc Molines[1]

[1]CNRS/LGGE (UMR 5183), Grenoble, France, [2]CERFACS/CNRS, URA1857, Toulouse, France, [3]CNES/LEGOS, Université Paul Sabatier, Toulouse, France

Abstract A global eddy-permitting (1/4° resolution) ocean general circulation model is shown to spontaneously generate intrinsic oceanic variability (IOV) up to multidecadal timescales ($T > 20$ years) under a repeated seasonal atmospheric forcing. In eddy-active regions, the signature of this multidecadal eddy-driven IOV on sea level is substantial, weakly autocorrelated, and is comparable to (and may clearly exceed) the corresponding signature of internal climate variability (ICV) produced by current coupled climate models—whose laminar ocean components may strongly underestimate IOV. Deriving sea level trends from finite-length time series in eddy-active regions yields uncertainties induced by this multidecadal IOV, which are of the same order of magnitude as those due to ICV. A white noise model is proposed to approximate the low-frequency tail of the IOV spectra and could be used to update ICV estimates from current climate simulations and projections.

1. Introduction

All climate projections based on results from coupled general circulation models (referred to as climate models hereafter) involved in the Coupled Model Intercomparison Project (CMIP5) indicate that sea level will rise faster and higher during the 21st century than during the 20th century under anthropogenic influence. However, the spread in projections of future sea level is substantial among CMIP5 climate models (more than ±50% of the ensemble mean for projections in 2080–2100 whichever the emission scenario [*Church et al.*, 2013]). This intermodel spread in sea level change is the combination of two kinds of uncertainty. The first one is induced by the chaos of the climate system and is thus irreducible: simulations performed with climate models are highly sensitive to initial conditions and are able to spontaneously generate variability without any external forcing, associated with phenomena such as the El Niño–Southern Oscillation. A consequence of this unforced variability, referred to as internal climate variability (ICV), is that CMIP5 climate models are not able to reproduce regional sea level variability with the same phase as the observations.

The second kind of uncertainty is related to the misrepresentation of certain physical processes in climate models such as sub–grid scale processes, including cloud microphysics and oceanic mesoscale eddies, as well as processes involved in the water cycle, including ice mass loss and freshwater fluxes from icebergs. The uncertainty in these processes may alter the simulation of global and regional sea level variability at multiple timescales [see also *Church et al.*, 2013]. Reducing these uncertainties requires either an increase in resolution or dedicated work on physical parameterizations and numerical schemes. An assessment of their impact on sea level change is also needed in comparison with observations. Such comparisons are, however, not straightforward because they require detecting sea level changes forced by external influences (anthropogenic, volcanic, and solar), above the noise induced by the ICV (this problem is generally referred to as the detection and attribution problem—D&A—in the literature [*Bindoff et al.*, 2013]). Hence, reducing the uncertainties due to the misrepresentation of the physics require a precise estimate of the first kind of uncertainty linked to the ICV.

So far, ICV has been estimated from climate model control simulations in which the external forcing of the climate system is held constant at preindustrial levels [*Slangen et al.*, 2014; *Richter and Marzeion*, 2014; *Carson et al.*, 2014; *Bilbao et al.*, 2015; *Lyu et al.*, 2015]. These simulations are run over centuries to millennia in order to get a robust estimate of ICV that could mask the forced signals. Unfortunately, because of common shortcomings in climate models, these simulations may not be sufficient to capture the (real) ICV of sea level.

In particular, the chaotic behavior of the turbulent ocean may be underestimated because most of the CMIP5 climate models do not resolve the oceanic mesoscale eddies and the associated nonlinear processes such as baroclinic instability [*Charney*, 1947; *Eady*, 1949; *Tulloch et al.*, 2011], the rectificitation of the mean or slowly varying flows [*Holland*, 1978; *Tai and White*, 1990; *Berloff*, 2005], and turbulence energy cascades [*Charney*, 1971; *Salmon*, 1998; *Scott and Wang*, 2005; *Arbic et al.*, 2012, 2014]. These oceanic eddies not only account for a substantial part of high-frequency oceanic variability, i.e., large-eddy kinetic energy [*Large et al.*, 1991; *Stammer and Wunsch*, 1999], but they may also affect longer-term variability. Eddying ocean global circulation models (OGCMs) have been shown to spontaneously generate low-frequency intrinsic oceanic variability (IOV) with a substantial imprint on sea level anomalies (SLAs) at interannual-to-decadal timescales [*Penduff et al.*, 2011; *Serazin et al.*, 2015]. At multidecadal timescales, IOV also imprints on SLA in some places of the Indian Ocean [*Li and Han*, 2015] as well as the Atlantic Meridional Overturning Circulation (AMOC) [*Gregorio et al.*, 2015]. Note that IOV derived for the forced eddying ocean is analogous to ICV for the whole climate system. Numerous idealized studied [e.g., *Dewar*, 2003; *Dijkstra and Ghil*, 2005; *Berloff et al.*, 2007; *Pierini*, 2011] and eddying OGCM experiments (see the comparison between the 2° laminar model and the 1/4° eddy-permitting model in *Penduff et al.* [2011]) have pointed out that resolving (at least partially) mesoscale eddies is necessary to simulate substantial levels of IOV.

In this paper, we focus on the imprint of eddy-driven multidecadal IOV on sea level over the global ocean, estimated using a 1/4° eddying OGCM driven by a mean climatological atmospheric cycle. We compare the magnitude of this multidecadal IOV to the multidecadal ICV inferred from the state-of-the-art climate models used in CMIP5, whose ocean components are laminar and may largely underestimate the contribution of oceanic eddies to the full ICV. Our objective is to determine whether the mere chaotic behavior of the turbulent ocean introduces a substantial noise (i.e., IOV) and should be taken into account in D&A studies. In order to fill the gap between climate models using laminar oceans (e.g., CMIP5) and future high-resolution climate models, we suggest that a white noise model could be applied to approximate multidecadal IOV in the regions where IOV is not autocorrelated at multidecadal timescales. Note that several recent studies [*Carson et al.*, 2014; *Bordbar et al.*, 2015] have quantified the ICV of sea level, estimated from CMIP5 models in terms of sea level trends (SLTs) over different periods. For the sake of comparison, we also propose here a quantification of the IOV in terms of trends over similar periods, which updates the uncertainty in SLTs computed with CMIP5 models.

2. Data and Methods

2.1. Simulations

We used the Nucleus for European Modeling of the Ocean (NEMO) [*Madec*, 2008] version 2.3 at 1/4° in the ORCA025 global configuration to perform a 327 year ocean-only simulation driven by a mean climatological atmospheric cycle repeated every year. This simulation, denoted as NEMO-Control, aims at isolating the IOV that spontaneously emerges from the eddying ocean. The climatological forcing function is derived from the Drakkar Forcing Set (DFS4) [*Brodeau et al.*, 2010] and yields a realistic mean state of the ocean [see *Penduff et al.*, 2011; *Gregorio et al.*, 2015]. The model uses a 46-level vertical discretization, a partial cell representation of topography, a momentum advection scheme that conserves energy and enstrophy [*Barnier et al.*, 2006; *Penduff et al.*, 2007; *Le Sommer et al.*, 2009], a total variance-diminishing tracer advection scheme, and an isopycnal Laplacian tracer diffusion operator. The vertical mixing scheme is based on the TKE turbulent closure model [*Blanke and Delecluse*, 1993], and the convective adjustment is handled by the enhancement of the vertical mixing in case of static instability. We use yearly and monthly mean SLA from the last 200 and 300 years of this eddying simulation, respectively. Note that the NEMO 1/4° configuration ORCA025 was shown to reasonably reproduce the large-scale patterns of SLTs compared to those observed from satellite altimetry over 1993–2001 [*Lombard et al.*, 2008].

We use the sea surface height above geoid from the noneddying preindustrial control simulations performed in the CMIP5 experiment [*Taylor et al.*, 2011]. The ensemble of these simulations is denoted here as CMIP5-Control. The preindustrial control simulations were performed without any externally induced variability (including anthropogenic) [*Taylor et al.*, 2009]. We choose to use the last 200 years of each CMIP5 simulations, the minimum length shared by all simulations.

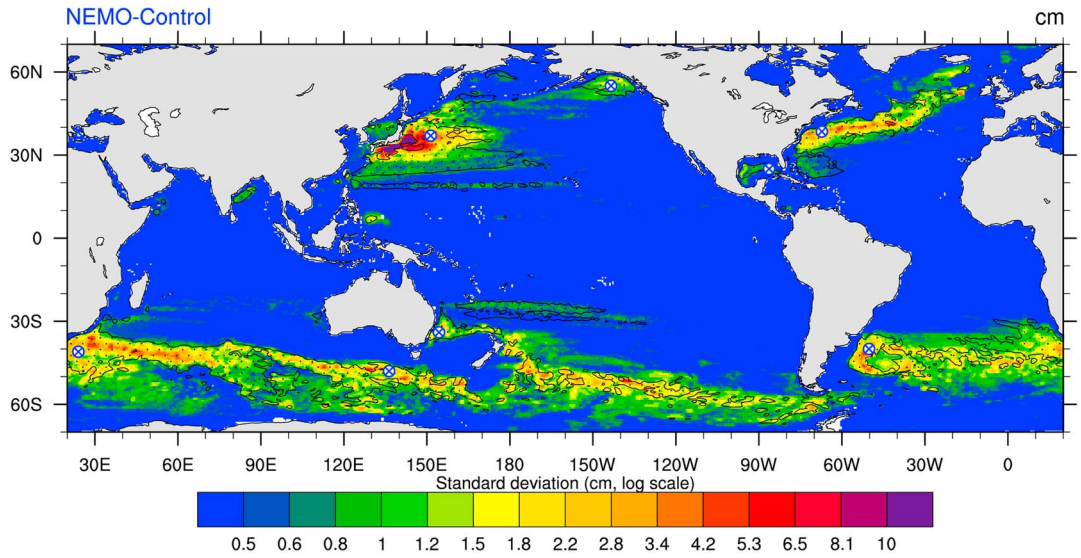

Figure 1. Standard deviation of the multidecadal (>20 years) SLA intrinsic variability in the 1/4° NEMO-Control simulation. Black contours correspond to short-term correlated time series ($\alpha < 0.65$). The blue crosses show the location of the time series used in Figure 3.

2.2. Time Series Processing and Analyses

For all simulations, global averages are first removed from yearly SLA maps. The nonlinear model drifts are removed from the time series by a high-pass filtering based on the nonparametric LOESS method [*Cleveland and Devlin*, 1988] (see examples illustrated in *Serazin et al.* [2015] and in *Gregorio et al.* [2015]). This nonlinear detrending is tuned here to remove signals with periods longer than 100 years from the 200 year time series. Then, a low-pass Lanczos filter [*Duchon*, 1979] with a cutoff period of 20 years is used to isolate the multidecadal timescales. These periods are not yet fully resolved in the existing 22 year altimetric record but may yield spurious regional SLTs. Our analysis also complements the study of *Serazin et al.* [2015] that characterized SLA intrinsic variability at interannual-to-decadal timescales (i.e., 1.5 to 20 years). The standard deviation $\sigma_{20\text{–}100\,\text{years}}$ is then computed from resulting SLA time series to quantify the amplitude of SLA variability on periods ranging from 20 to 100 years.

We apply the Detrended Fluctuations Analysis (DFA) to estimate the power law decay of the autocorrelation function of time series [*Kantelhardt et al.*, 2001], i.e., the time series memory. DFA is a variation of the Hurst Exponent technique, used in the analysis of nonstationary time series, and has been applied to demonstrate the long-term persistence in sea level records [*Dangendorf et al.*, 2014]. The DFA exponent α is directly linked to the slope of the power spectrum $P(\omega)$ by the relation $P(\omega) \sim \omega^{1-2\alpha}$, where ω denotes the temporal frequency. A white spectrum, i.e., an uncorrelated or short-term memory time series, corresponds to a value $\alpha = 0.5$. Long-term-correlated and nonstationary time series are respectively characterized by $0.5 < \alpha < 1$ (pink noise) and by $\alpha > 1$ (random walk, red noise). DFA is applied on the last 300 years of monthly outputs from NEMO-Control.

In order to provide an estimate of the low-frequency tail of the IOV spectrum for the D&A of regional sea level change, we suggest a simple white noise model $W(\omega)$ for the regions where NEMO-Control time series are short-term correlated (i.e., $\alpha < 0.65$). The Parserval theorem states that the variance of the band-passed time series $\text{SLA}_{20\text{–}100\,\text{years}}(t)$ is equal to the integral of the power density spectra between 1/20 cpy and 1/100 cpy, so that the white noise power spectrum density $W(\omega)$ must verify

$$\sigma_{20\text{–}100\,\text{years}}{}^2 = \int_0^{200} \|\text{SLA}_{20\text{–}100\,\text{years}}(t)\|^2 \mathrm{d}t = \int_{1/100}^{1/20} W(\omega')\mathrm{d}\omega'. \quad (1)$$

Because $W(\omega)$ is characterized by a constant power spectrum density, the integral of the rightmost term is trivial and leads to

$$W(\omega) = 25\,\sigma_{20\text{–}100\,\text{years}}{}^2. \quad (2)$$

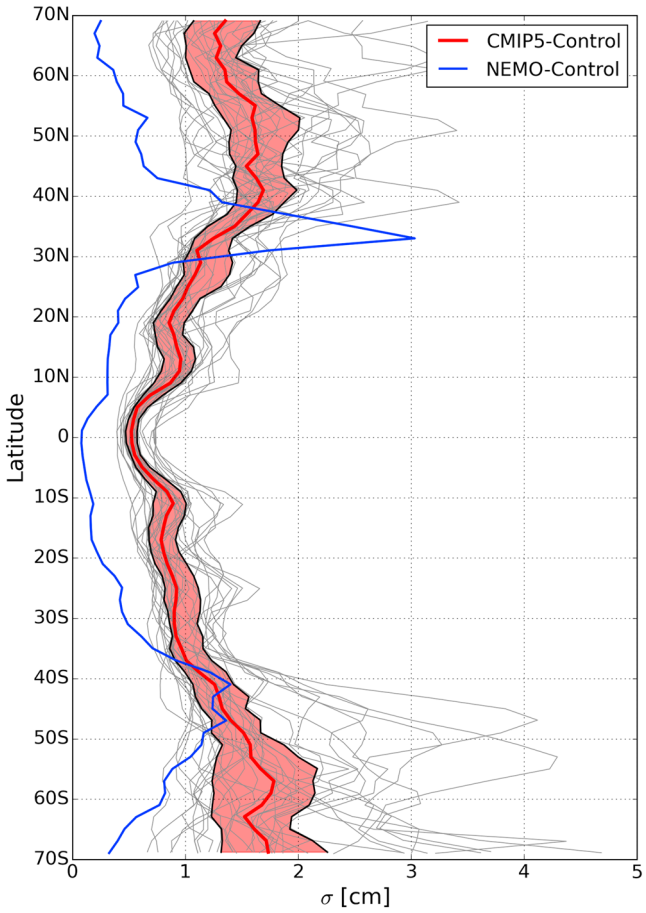

Figure 2. Zonal average of the standard deviation of the multidecadal (> 20 years) SLA intrinsic variability in the 1/4° NEMO-Control simulation (blue) and in the ensemble of coupled simulations CMIP5-Control (grey and red). Each CMIP5 simulation is plotted in grey, the median of the ensemble is represented by the red line, and the area between the 25th and 75th percentiles is filled in red.

Thus, such a spectrum may be directly derived from the multidecadal variance map of IOV inferred from NEMO-Control (see Figure 1).

To check whether $W(\omega)$ is representative of the multidecadal IOV, we perform a spectral analysis at eight different locations where multidecadal IOV is substantial and has short-term memory in NEMO-Control (i.e., large $\sigma_{20\text{-}100\,\text{years}}$ and $\alpha < 0.65$). The spectra are computed over 200 years with a 100 year wide Hanning window and an overlap of 50%. The zero-padding method is used to improve the spectral resolution. We repeat the computation for each of the CMIP5-Control simulations to compare ICV and IOV spectra.

Multidecadal ICV may induce spurious regional SLTs when they are derived from finite-length time series (e.g., from altimetry or tide gauges). Internally induced regional SLTs may be seen as representing uncertainties on the detection of anthropogenic forcing and on projections of sea level changes [*Hu and Deser*, 2013; *Carson et al.*, 2014]. Here we quantify the eddy-related uncertainties induced by multidecadal IOV following *Carson et al.* [2014] for the ICV on 19 simulations of CMIP5-Control: we compute the root-mean-square (RMS) spread in 20 year regional SLTs in overlapping segments, starting every 5 years, and extracted from the detrended 300 year NEMO-Control time series. The same RMS computation is reiterated for successive 50 year and 100 year segments.

3. Results

The NEMO-Control simulation, which isolates the IOV, exhibits substantial SLA standard deviation at multidecadal timescales (20–100 years) in eddy-active regions (Figure 1), mainly in the Western Boundary Currents (WBCs) and in the Antarctic Circumpolar Current (ACC). The eddying ocean thus spontaneously generates

substantial multidecadal IOV in these regions. This standard deviation $\sigma_{20-100\text{years}}$ is maximum (~10 cm) in the Kuroshio; reaches 3–4 cm in the Gulf Stream, the Malvinas current, the East Australian Current, the Agulhas current, and the ACC; and is about 1 cm in the Gulf of Alaska, the Gulf of Mexico, the Japan Sea, and the Bay of Bengal. Equatorial regions do not exhibit substantial multidecadal IOV in sea level, consistent with the previous results of *Penduff et al.* [2011] and *Serazin et al.* [2015] who showed negligible interannual-to-decadal IOV in these regions.

Figure 2 shows $\sigma_{20-100\,\text{years}}$ from NEMO-Control (eddy-driven IOV, blue line) as a zonal average, along with its counterpart due to the coupled ICV (CMIP5-Control, red line); in the latter, multidecadal SLA variability is due either to atmospheric forcing or to air-sea coupling, but not to the (unresolved) oceanic mesoscale eddies. The zonally averaged impact of multidecadal eddy-driven IOV on SLA clearly exceeds that of the CMIP5 coupled ICV between 30 and 38°N, i.e., at the latitudes of the Gulf Stream and Kuroshio extensions. In the ACC latitudinal range (37–49°S), the climatological eddying ocean simulation (NEMO-Control) and CMIP5 models spontaneously generate similar amounts of 20–100 year variability. The eddy-driven IOV is comparable and sometimes exceeds the CMIP5-coupled ICV within most of the eight eddy-active regions shown in Figure 1 (see the power density spectra in Figure 3), in particular in the Agulhas countercurrent, around the Zapiola anticyclone and in the Gulf of Mexico. In summary, CMIP5 models are very likely to underestimate the imprint of multidecadal ICV on SLAs in midlatitude eddy-active regions because they do not resolve oceanic mesoscale eddies, which spontaneously generate substantial low-frequency variability.

The DFA performed on NEMO-Control yields α exponents that do not exceed 0.65 within the black contours shown in Figure 1. Most of these areas correspond to eddy-active regions with substantial multidecadal IOV and are thus characterized by short-term memory processes, i.e., not correlated at multidecadal timescales. Such α values are consistent with the whitening of the IOV spectra at interannual to multidecadal timescales (Figure 3), except in the ACC. In this region, the spectral slope is nonzero at interannual timescales (i.e., autocorrelated time series) but the DFA analysis suggests that the slope is likely to flatten at multidecadal timescales. This difference might be explained by spontaneous low-frequency modulations of local jets interacting with the topography [*Thompson and Richards*, 2011]. The white noise model $W(\omega)$ (dashed blue curve), inferred from the SLA variance map (Figure 1), therefore provides a reasonable approximation of the low-frequency tail of the IOV spectra for most of the regions studied (Figure 3). Unlike in NEMO-Control, the ICV spectra derived from CMIP5 simulations have long-term memory, i.e., nonzero spectral slope, probably because mesoscale processes are not resolved. The oceanic eddy activity is indeed likely to produce large SLA signals that rapidly decorrelate in time. These intrinsic signals may overcome the weaker, long-term correlated response to wind and buoyancy forcing over a wide range of timescales up to multidecadal. We may expect that the next generation of coupled models with eddy-permitting oceans will have similarly flat kinetic energy spectra at low-frequency in eddy-active regions.

Multidecadal IOV yields uncertainties on regional SLT estimates computed from finite-length time series. These uncertainties are quantified over three typical periods in Figure 4. The uncertainties on SLA trends evaluated from 20 year time series (duration of the altimetric record, Figure 4 (top)) may actually exceed 3 mm/yr in the Kuroshio, the Gulf Stream, and the ACC regions. Except in the Kuroshio, these uncertainties fall below 1 mm/yr when regional SLTs are evaluated over 50 years, and below 0.4 mm/yr over 100 years. SLT uncertainties induced by the eddy-driven IOV (Figure 4) are therefore comparable to those induced by the coupled ICV estimated from CMIP5 laminar ocean simulations [see *Carson et al.*, 2014, Figures 2–4].

4. Discussion

The results presented in this paper show that the imprint of IOV on SLA reaches substantial levels at multidecadal timescales in the eddying regime, i.e., when mesoscale eddies are (even partially) resolved. This principally concerns eddy-active regions where SLA time series are not correlated at multidecadal timescales. Our estimate of IOV is comparable to (and sometimes larger than) the ICV simulated in the CMIP5 experiments, which argues that current coupled climate models using laminar ocean components (e.g., CMIP5) may underestimate this eddy-induced source of low-frequency oceanic variability (i.e., the oceanic chaos). The use of laminar oceans in coupled models may therefore yield underestimated levels of internal SLA variance, which is a serious drawback for D&A studies. To overcome this drawback, we suggest a simple stochastic representation of this eddy-induced IOV by using a white noise model at multidecadal timescales in eddy-active regions. This stochastic model may be used to update the estimates of SLT uncertainties deduced from laminar ocean

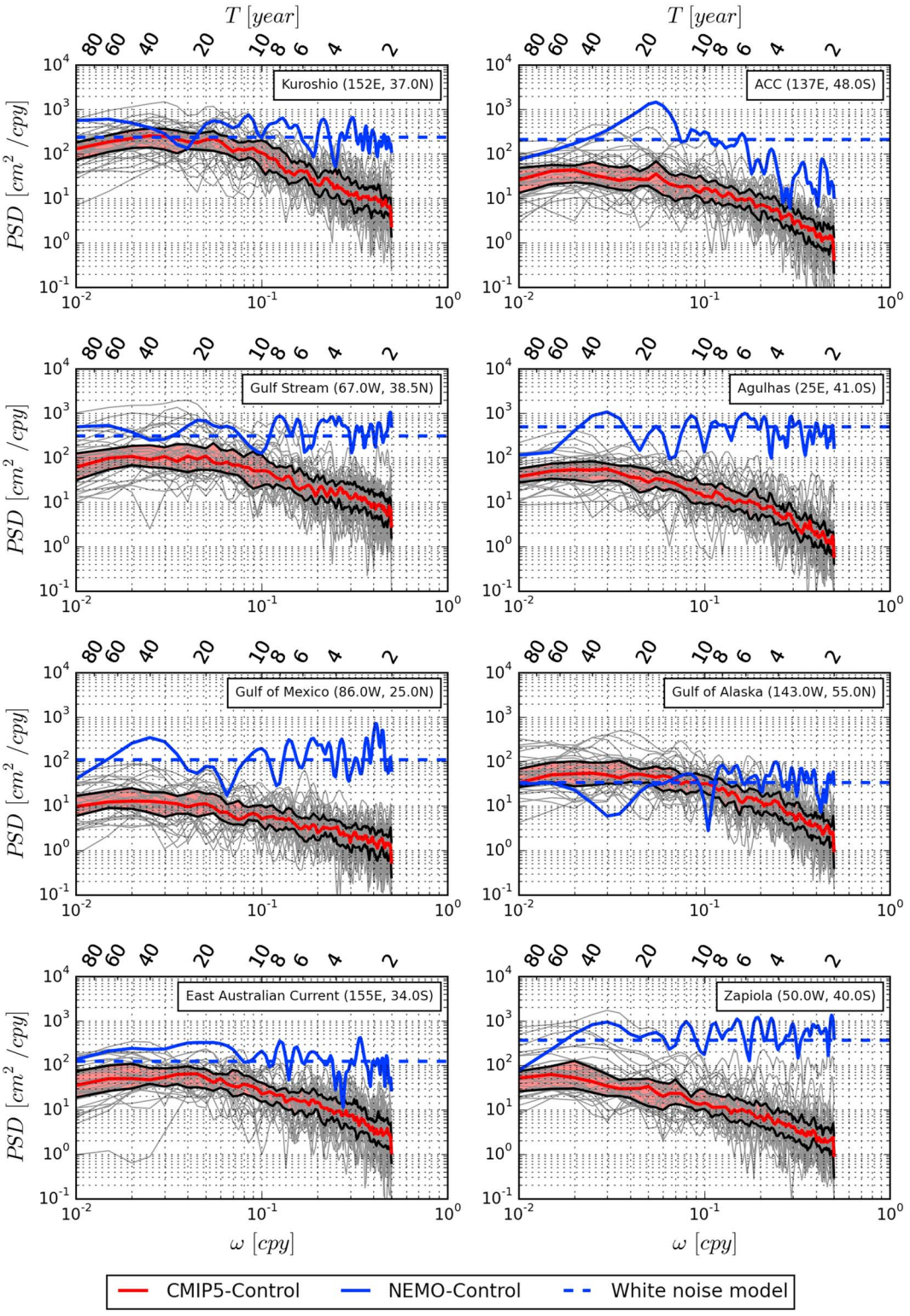

Figure 3. Power spectrum densities of SLA at interannual to multidecadal timescales in eight eddy-active regions computed on the ocean-only NEMO-Control simulation (blue) and on the ensemble of coupled simulations CMIP5-Control (grey and red). A white noise model (dashed blue curve) is estimated from the variance of the low-passed time series denoted by the blue crosses in Figure 1. Spectra are computed over 200 year time series using a 100 year wide Hanning window with 50% overlap and the zero-padding method is used to improve the spectrum resolution.

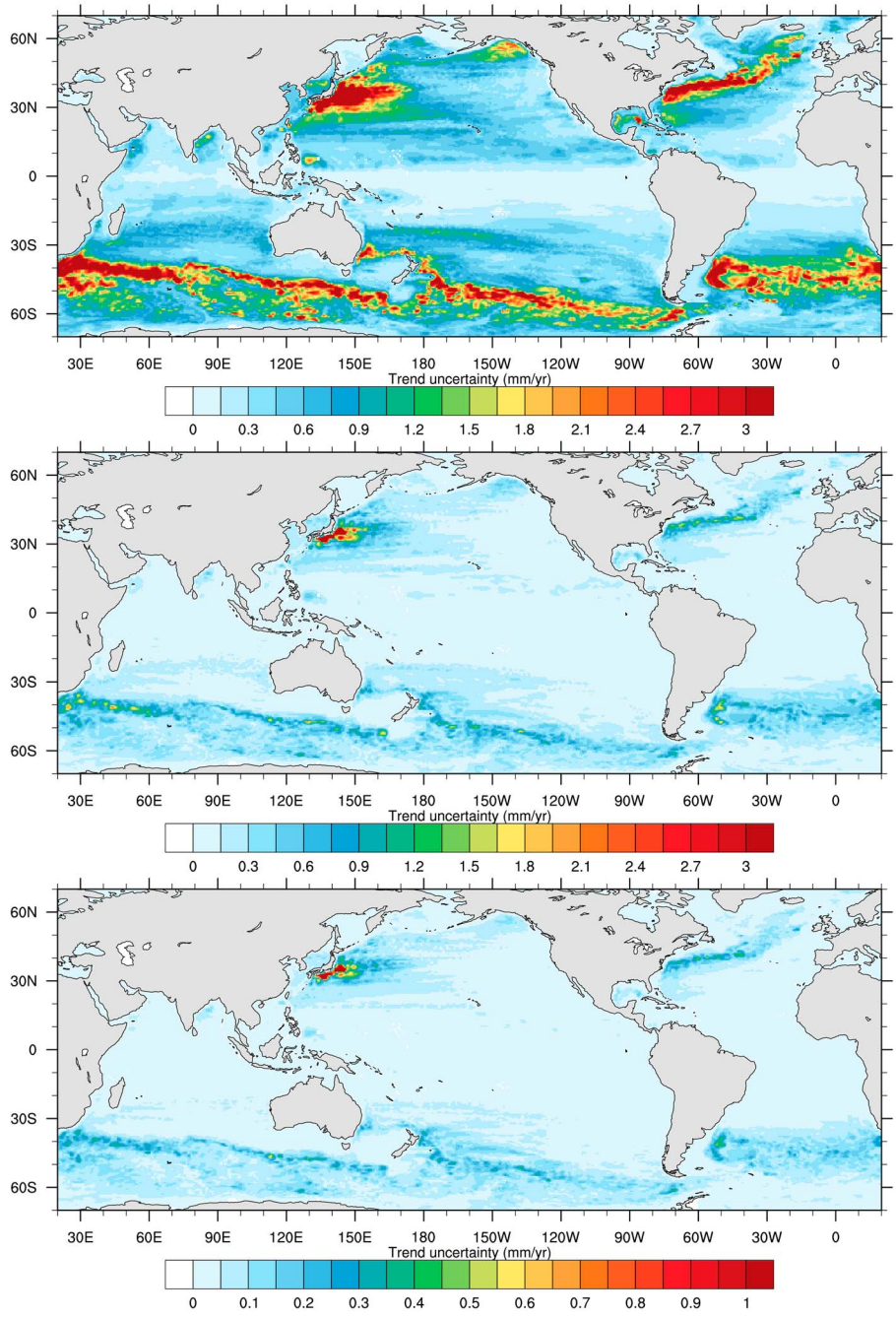

Figure 4. RMS error of regional sea level trends evaluated on (top) 20 year, (middle) 50 year, and (bottom) 100 year consecutive segments from the 1/4° NEMO-Control simulation.

coupled models (e.g., CMIP5 experiments), as we wait for the future generations of climate models that will explicitly resolve (at least partially) oceanic eddies and will be probably more realistic in terms of internally induced SLA variability levels.

Multidecadal IOV was estimated from an eddy-permitting forced 1/4° OGCM, which resolves mesoscale eddies only partially. Should we expect an increase of intrinsic multidecadal SLA variance at finer ocean model resolution? Using a 70 year 1/12° eddy-resolving OGCM, forced by a repeated climatological cycle, *Serazin et al.* [2015] showed that the 1.5–20 year IOV increases by a substantial amount in midlatitude regions when resolution increases from 1/4° to 1/12°. This increase in interannual-to-decadal variability is consistent with an increase in mesoscale activity in the 1/12° model. A spectral analysis (unpublished) recently confirms

this resolution-induced increase at interannual timescales, but not at decadal and longer timescales where 1/4° and 1/12° simulations yield comparable IOV levels. *Gregorio et al.* [2015] also report similar AMOC IOV levels when switching from the 1/4° to the 1/12° resolution. Our 327 year 1/4° simulation might thus provide a reasonable (lower) estimate of the multidecadal intrinsic SLA variance compared to a higher resolution (but shorter) 1/12° simulation; verifying this statement would require that we integrate the 1/12° eddy-resolving OGCM over centuries, which would better assess the multidecadal intrinsic SLA variability, but at a huge computational cost. In particular, our low-frequency IOV might be underestimated in regions where deformation radii are small and poorly resolved at 1/4° (e.g., Mediterranean Sea and Japan Sea).

The nonlinear processes involved in the generation of IOV are still poorly known in realistic ocean models and are a topic of active research. *Arbic et al.* [2012, 2014] have shown that nonlinear advection of relative vorticity may spontaneously transfer geostrophic kinetic energy from high to lower frequencies. Yet those nonlinear scale interactions might not transfer energy to timescales longer than interannual or decadal according to a similar analysis performed by the author on a 1/12° climatological simulation (not shown here). Other mechanisms involving the rectification by oceanic eddies of eastward jets in WBC systems [*Dewar*, 2003; *Berloff et al.*, 2007] and ACC jets [*Hogg and Blundell*, 2006] or transitions between basin-scale modes through Hopf and homoclinic bifurcations [*Dijkstra and Ghil*, 2005; *Pierini*, 2011] have been suggested in process-oriented studies to explain the spontaneous generation of low-frequency IOV in the ocean; only a few studies have attempted to explore these mechanisms in realistic OGCMs [e.g., *Taguchi et al.*, 2010; *Thompson and Richards*, 2011]. Exploring such mechanisms would yield a better understanding of intrinsic sea level spectra, especially in the ACC where we have found a different behavior at interannual timescales.

Acknowledgments
We thank Rosemary Morrow for interesting discussions and two anonymous reviewers for their constructive remarks that helped to improve this article. We thank Sönke Dangendorf for sharing the DFA algorithm and for fruitful discussions on the interpretation of the results. The CMIP5 data are available through the portal, the Earth System Grid-Center for Enabling Technologies (ESG-CET), on the page http://pcmdi9.llnl.gov/. The NEMO-Control data are available by directly contacting the main author by mail at guillaume.serazin@lgge.obs.ujf-grenoble.fr. The NEMO-Control data are stored for several years according to the DRAKKAR data policy. This work is a contribution to the CHAOCEAN and OCCIPUT projects. It benefited from the DRAKKAR international coordination network (GDRI) established between CNRS, NOCS, GEOMAR, and IFREMER. For this work, DRAKKAR also benefited from a grant from GMMC through the LEFE program of INSU. CHAOCEAN is supported by the Centre National d'Études Spatiales (CNES) through the Ocean Surface Topography Science Team (OST/ST). OCCIPUT is supported by the ANR through contract ANR-13-BS06-0007-01. The computations presented in this study were performed at CINES under the allocation made by GENCIx2013010727. The ORCA12-GJM02 simulation was performed as part of the Grands Challenges GENCI/CINES 2013. G.S. is supported by CNES and Région Midi-Pyrénées; T.P., B.B., and J.M.M. by CNRS; and L.T. by CERFACS.

References

Arbic, B. K., R. B. Scott, G. R. Flierl, A. J. Morten, J. G. Richman, and J. F. Shriver (2012), Nonlinear cascades of surface oceanic geostrophic kinetic energy in the frequency domain, *J. Phys. Oceanogr.*, *42*(9), 1577–1600, doi:10.1175/JPO-D-11-0151.1.

Arbic, B. K., M. Müller, J. G. Richman, J. F. Shriver, A. J. Morten, R. B. Scott, G. Serazin, and T. Penduff (2014), Geostrophic turbulence in the frequency-wavenumber domain: Eddy-driven low-frequency variability, *J. Phys. Oceanogr.*, *44*(8), 2050–2069, doi:10.1175/JPO-D-13-054.1.

Barnier, B., et al. (2006), Impact of partial steps and momentum advection schemes in a global ocean circulation model at eddy-permitting resolution, *Ocean Dyn.*, *56*(5-6), 543–567, doi:10.1007/s10236-006-0082-1.

Berloff, P. S. (2005), On rectification of randomly forced flows, *J. Mar. Res.*, *63*(3), 497–527, doi:10.1357/0022240054307894.

Berloff, P. S., A. M. Hogg, and W. Dewar (2007), The turbulent oscillator: A mechanism of low-frequency variability of the wind-driven ocean gyres, *J. Phys. Oceanogr.*, *37*(9), 2363–2386, doi:10.1175/JPO3118.1.

Bilbao, R. A. F., J. M. Gregory, and N. Bouttes (2015), Analysis of the regional pattern of sea level change due to ocean dynamics and density change for 1993–2099 in observations and CMIP5 AOGCMs, *Clim. Dyn.*, *45*(9-10), 2647–2666, doi:10.1007/s00382-015-2499-z.

Bindoff, N., et al. (2013), Detection and attribution of climate change: From global to regional, in *Climate Change 2013: The Physical Science Basis. Contribution of Working Group I to the Fifth Assessment Report of the Intergovernmental Panel on Climate Change*, edited by T. Stocker et al., pp. 867–952, Cambridge Univ. Press, Cambridge, U. K., and New York.

Blanke, B., and P. Delecluse (1993), Variability of the tropical Atlantic ocean simulated by a general circulation model with two different mixed-layer physics, *J. Phys. Oceanogr.*, *23*(7), 1363–1388, doi:10.1175/1520-0485(1993)023<1363:VOTTAO>2.0.CO;2.

Bordbar, M. H., T. Martin, M. Latif, and W. Park (2015), Effects of long-term variability on projections of twenty-first century dynamic sea level, *Nat. Clim. Change*, *5*(4), 343–347, doi:10.1038/nclimate2569.

Brodeau, L., B. Barnier, A.-M. Treguier, T. Penduff, and S. Gulev (2010), An ERA40-based atmospheric forcing for global ocean circulation models, *Ocean Model.*, *31*(3–4), 88–104, doi:10.1016/j.ocemod.2009.10.005.

Carson, M., A. Köhl, and D. Stammer (2014), The impact of regional multidecadal and century-scale internal climate variability on sea level trends in CMIP5 models, *J. Clim.*, *28*(2), 853–861, doi:10.1175/JCLI-D-14-00359.1.

Charney, J. G. (1947), The dynamics of long waves in a baroclinic westerly current, *J. Meteorol.*, *4*(5), 136–162, doi:10.1175/1520-0469(1947)004<0136:TDOLWI>2.0.CO;2.

Charney, J. G. (1971), Geostrophic turbulence, *J. Atmos. Sci.*, *28*(6), 1087–1095, doi:10.1175/1520-0469(1971)028<1087:GT>2.0.CO;2.

Church, J., et al. (2013), Sea level change, in *Climate Change 2013: The Physical Science Basis. Contribution of Working Group I to the Fifth Assessment Report of the Intergovernmental Panel on Climate Change*, edited by T. Stocker et al., pp. 1137–1216, Cambridge Univ. Press, Cambridge, U. K., and New York.

Cleveland, W. S., and S. J. Devlin (1988), Locally weighted regression: An approach to regression analysis by local fitting, *J. Am. Stat. Assoc.*, *83*(403), 596–610, doi:10.2307/2289282.

Dangendorf, S., D. Rybski, C. Mudersbach, A. Müller, E. Kaufmann, E. Zorita, and J. Jensen (2014), Evidence for long-term memory in sea level, *Geophys. Res. Lett.*, *41*, 5530–5537, doi:10.1002/2014GL060538.

Dewar, W. K. (2003), Nonlinear midlatitude ocean adjustment, *J. Phys. Oceanogr.*, *33*(5), 1057–1082, doi:10.1175/1520-0485(2003)033<1057:NMOA>2.0.CO;2.

Dijkstra, H. A., and M. Ghil (2005), Low-frequency variability of the large-scale ocean circulation: A dynamical systems approach, *Rev. Geophys.*, *43*, RG3002, doi:10.1029/2002RG000122.

Duchon, C. (1979), Lanczos filtering in one and 2 dimensions, *J. Appl. Meteorol.*, *18*(8), 1016–1022, doi:10.1175/1520-0450(1979)018<1016:LFIOAT>2.0.CO;2.

Eady, E. T. (1949), Long waves and cyclone waves, *Tellus*, *1*(3), 33–52, doi:10.1111/j.2153-3490.1949.tb01265.x.

Gregorio, S., T. Penduff, G. Serazin, J.-M. Molines, B. Barnier, and J. Hirschi (2015), Intrinsic variability of the Atlantic meridional overturning circulation at interannual-to-multidecadal timescales, *J. Phys. Oceanogr.*, *45*, 1929–1946, doi:10.1175/JPO-D-14-0163.1.

Hogg, A. M., and J. R. Blundell (2006), Interdecadal variability of the Southern Ocean, *J. Phys. Oceanogr.*, *36*(8), 1626–1645, doi:10.1175/JPO2934.1.
Holland, W. R. (1978), The role of mesoscale eddies in the general circulation of the ocean-numerical experiments using a wind-driven quasi-geostrophic model, *J. Phys. Oceanogr.*, *8*(3), 363–392, doi:10.1175/1520-0485(1978)008<0363:TROMEI>2.0.CO;2.
Hu, A., and C. Deser (2013), Uncertainty in future regional sea level rise due to internal climate variability, *Geophys. Res. Lett.*, *40*(11), 2768–2772, doi:10.1002/grl.50531.
Kantelhardt, J. W., E. Koscielny-Bunde, H. A. Rego, S. Havlin, and A. Bunde (2001), Detecting long-range correlations with detrended fluctuation analysis, *Physica A*, *295*(3-4), 441–454, doi:10.1016/S0378-4371(01)00144-3.
Large, W. G., W. R. Holland, and J. C. Evans (1991), Quasi-geostrophic ocean response to real wind forcing: The effects of temporal smoothing, *J. Phys. Oceanogr.*, *21*(7), 998–1017, doi:10.1175/1520-0485(1991)021<0998:QGORTR>2.0.CO;2.
Le Sommer, J., T. Penduff, S. Theetten, G. Madec, and B. Barnier (2009), How momentum advection schemes influence current-topography interactions at eddy permitting resolution, *Ocean Model.*, *29*(1), 1–14, doi:10.1016/j.ocemod.2008.11.007.
Li, Y., and W. Han (2015), Decadal sea level variations in the Indian Ocean investigated with HYCOM: Roles of climate modes, ocean internal variability, and stochastic wind forcing, *J. Clim.*, *28*, 9143–9165, doi:10.1175/JCLI-D-15-0252.1.
Lombard, A., G. Garric, and T. Penduff (2008), Regional patterns of observed sea level change: Insights from a 1/4 global ocean/sea-ice hindcast, *Ocean Dyn.*, *59*(3), 433–449, doi:10.1007/s10236-008-0161-6.
Lyu, K., X. Zhang, J. A. Church, and J. Hu (2015), Quantifying internally generated and externally forced climate signals at regional scales in CMIP5 models, *Geophys. Res. Lett.*, *42*, 9394–9403, doi:10.1002/2015GL065508.
Madec, G. (2008), *NEMO Ocean Engine, Note du Pole de modélisation 27*, Institut Pierre-Simon Laplace (IPSL), France.
Penduff, T., J. Le Sommer, B. Barnier, A.-M. Treguier, J. Molines, and G. Madec (2007), Influence of numerical schemes on current-topography interactions in 1/4 degrees global ocean simulations, *Ocean Sci.*, *3*(4), 509–524.
Penduff, T., M. Juza, B. Barnier, J. Zika, W. K. Dewar, A.-M. Treguier, J.-M. Molines, and N. Audiffren (2011), Sea level expression of intrinsic and forced ocean variabilities at interannual time scales, *J. Clim.*, *24*(21), 5652–5670, doi:10.1175/JCLI-D-11-00077.1.
Pierini, S. (2011), Low-frequency variability, coherence resonance, and phase selection in a low-order model of the wind-driven ocean circulation, *J. Phys. Oceanogr.*, *41*(9), 1585–1604, doi:10.1175/JPO-D-10-05018.1.
Richter, K., and B. Marzeion (2014), Earliest local emergence of forced dynamic and steric sea-level trends in climate models, *Environ. Res. Lett.*, *9*(11), 114009, doi:10.1088/1748-9326/9/11/114009.
Salmon, R. (1998), *Lectures on Geophysical Fluid Dynamics*, Oxford Univ. Press. [Available at https://global.oup.com/academic/product/lectures-on-geophysical-fluid-dynamics-9780195108088.]
Scott, R. B., and F. Wang (2005), Direct evidence of an oceanic inverse kinetic energy cascade from satellite altimetry, *J. Phys. Oceanogr.*, *35*(9), 1650–1666, doi:10.1175/JPO2771.1.
Slangen, A. B. A., J. A. Church, X. Zhang, and D. Monselesan (2014), Detection and attribution of global mean thermosteric sea level change, *Geophys. Res. Lett.*, *41*, 5951–5959, doi:10.1002/2014GL061356.
Stammer, D., and C. Wunsch (1999), Temporal changes in eddy energy of the oceans, *Deep Sea Res. Part II*, *46*(1-2), 77–108, doi:10.1016/S0967-0645(98)00106-4.
Serazin, G., T. Penduff, S. Gregorio, B. Barnier, J.-M. Molines, and L. Terray (2015), Intrinsic variability of sea level from global ocean simulations: Spatiotemporal scales, *J. Clim.*, *28*(10), 4279–4292, doi:10.1175/JCLI-D-14-00554.1.
Taguchi, B., B. Qiu, M. Nonaka, H. Sasaki, S.-P. Xie, and N. Schneider (2010), Decadal variability of the Kuroshio Extension: Mesoscale eddies and recirculations, *Ocean Dyn.*, *60*(3), 673–691, doi:10.1007/s10236-010-0295-1.
Tai, C.-K., and W. B. White (1990), Eddy variability in the Kuroshio extension as revealed by Geosat Altimetry: Energy propagation away from the jet, Reynolds stress, and seasonal cycle, *J. Phys. Oceanogr.*, *20*(11), 1761–1777, doi:10.1175/1520-0485(1990)020<1761:EVITKE>2.0.CO;2.
Taylor, K. E., R. J. Stouffer, and G. A. Meehl (2009), A summary of the CMIP5 experiment design, PCMDI Tech. Rep., p. 33, World Climate Research Program (WCRP). [Available at http://cmip-pcmdi.llnl.gov/cmip5/docs/Taylor_CMIP5_design.pdf.]
Taylor, K. E., R. J. Stouffer, and G. A. Meehl (2011), An overview of CMIP5 and the experiment design, *Bull. Am. Meteorol. Soc.*, *93*(4), 485–498, doi:10.1175/BAMS-D-11-00094.1.
Thompson, A. F., and K. J. Richards (2011), Low frequency variability of Southern Ocean jets, *J. Geophys. Res.*, *116*, C09022, doi:10.1029/2010JC006749.
Tulloch, R., J. Marshall, C. Hill, and K. S. Smith (2011), Scales, growth rates, and spectral fluxes of baroclinic instability in the ocean, *J. Phys. Oceanogr.*, *41*(6), 1057–1076, doi:10.1175/2011JPO4404.1.